



Chattering reduction effect on power efficiency of IFOC based induction motor

Dedid Cahya Happyanto^{1*}, Angga Wahyu Aditya²

¹Departemen Teknik Elektro, Politeknik Elektronika Negeri Surabaya

²Jurusan Teknik Elektro, Politeknik Negeri Balikpapan

¹Jl. Raya ITS – Keputih – Sukolilo, Kota Surabaya (60111) – East Java, Indonesia

²Jl. Soekarno Hatta Km. 8 – Batu Ampar, Kota Balikpapan (76129) – East Kalimantan, Indonesia

*Corresponding Email : dedid@pens.ac.id

Received 10 January 2022, Revised 09 April 2022, Accepted 17 May 2022

Abstract — The vector control strategies have developed rapidly and significantly to control Induction Motor (IM) compared to scalar control strategies. It causes better performance in managing IM. Indirect Field Oriented Control (IFOC) is one of the vector control strategies which more realistic to apply in the industrial world. However, IFOC requires Sliding Mode Control (SMC) with the Lyapunov function to ensure robustness and stability. Unfortunately, the first-order SMC or ordinary SMC has disadvantages in the chattering phenomenon. It uses boundary layer techniques to overcome the chattering phenomenon. This paper shows the analyzed boundary layer performance on rotor speed response, stator current response in the dq0 frame, and power performance. The SMC with and without boundary layer has an error steady-state less than 2% in rotor speed response. In stator current response with dq0 frame, the boundary layer with hyperbolic tangent function has the best performance. The power analysis shows that the boundary layer with saturation function has an active power loss of 39.16%, reactive power loss of 23.37%, and apparent power loss of 30.30%. The boundary layer with hyperbolic tangent functions has the best performance in reducing power consumption with an active power loss of 41.24%, reactive power loss of 24.78%, and apparent power loss of 31.96%.

Keywords – Induction Motors, IFOC, Chattering Reduction, SMC, Power Efficiency

Copyright © 2022 JURNAL INFOTEL

All rights reserved.

I. INTRODUCTION

The use of IM today has covered various aspects. In transportation, Tesla Model S and other electric vehicles use IM for the main engine [1], [2]. In industrial automation, traction machines and photovoltaic pumps utilize the IM [3], [4]. Furthermore, the IM is used as a propulsion engine for military purposes [5]. IM has many advantages, especially in durability, low cost, ease of maintenance, and a highly efficient electric motor. However, IM is hard to control. The standard control techniques of IM are scalar control and vector control. The scalar control principal principle of IM is based on the varying frequency and absolute values of voltages, currents, and interlinkages of windings [6], [7]. The scalar control is easy to use and implement. However, it has low-performance a low-performance

[8], [9]. Vector control principle represents the complicated IM model similarly DC motor. The vector control provides high efficiency in a wide speed range, decoupled control of torque and flux, four-quadrant operation, and better dynamic behavior than scalar control [10], [11].

Field Oriented Control (FOC) techniques are the vector control method that decouples electromagnetic torque and flux of an IM similar to the DC motor to obtain a good performance. IFOC is a FOC technique that can be more implemented and accepted by the industry than Direct FOC (DFOC) because the DFOC needs a flux sensor mounted in the air gap of IM [12]. In IFOC, the rotor flux is estimated using the field-oriented control equations.

IFOC requires controllers to guarantee robustness and stability against disturbances [13], [14], [15]. The

controller method can be classified into a model-free and a model-based controller. A model-free controller doesn't need a dynamic model in generated control signal [16], [17], [18]. A Model-based controller such as SMC is designed based on IFOC mathematical model for IM. SMC guarantees robustness and stability using the Lyapunov function. However, ordinary SMC has disadvantages in the chattering phenomenon that it consumes more energy and harms the hardware. The boundary layer limits chattering on SMC due to the discontinuous control input.

In this paper, IFOC-based IM is designed with SMC using sign function in flux controller, current regulator, and speed controller. The speed controller is designed with the boundary layer using saturation and hyperbolic tangent functions to overcome the chattering phenomenon. Analysis of power consumption and dynamic response is used to determine the performance of the sign function, saturation function, and hyperbolic tangent function.

II. RESEARCH METHOD

A. IFOC Based IM

IM mathematical models consist of electrical and mechanical models electrical and mechanical models. The rotor speed and rotor flux equation are mechanical models, while the current regulator is an electrical model. The state-space representation of IM models in the the direct-quadrature-zero rotating frame (dq0 frame) shows in (1) [11]. The IM models in the dq0 frame are derived from the IM equation in the ABC frame with Clarke and park transform.

$$\dot{X} = AX + BU \quad (1)$$

Where :

A =

$$\begin{bmatrix} -R_x/\sigma L_s & \omega_s & R_r L_m/L_r^2 \sigma L_s & L_m \omega_r/L_r \\ \omega_s & -R_x/\sigma L_s & L_m \omega_r/L_r & R_r L_m/L_r^2 \sigma L_s \\ L_m/T_r & 0 & -1/T_r & \omega_{sl} \\ 0 & L_m/T_r & \omega_{sl} & -1/T_r \end{bmatrix}$$

$$X = \begin{bmatrix} i_{ds} \\ i_{qs} \\ \varphi_{rd} \\ \varphi_{rq} \end{bmatrix}; B = \begin{bmatrix} 1/\sigma L_s \\ 1/\sigma L_s \\ 0 \\ 0 \end{bmatrix}; U = \begin{bmatrix} V_{ds} \\ V_{qs} \\ 0 \\ 0 \end{bmatrix}$$

where:

V_{ds}, V_{qs} : stator voltage in dq0 frame

i_{ds}, i_{qs} : stator current in dq0 frame

$\varphi_{rd}, \varphi_{rq}$: rotor flux in dq0 frame

ω_s : stator speed

R_r : rotor resistance

R_s : stator resistance

L_r : rotor inductance
 L_s : stator inductance
 L_m : mutual inductance
 P : number of pole pairs
 with:

$$R_x = R_s + \frac{L_m^2}{L_r^2} R_r$$

$\omega_{sl} = \omega_s - \omega_r$: slip calculation

$T_r = L_r/R_r$: rotor time constant

$\sigma = 1 - \frac{L_m^2}{(L_s + L_r)}$: total leakage factor

The mechanical model of the IM is expressed in (2).

$$\frac{d\omega_r}{dt} = \frac{L_m}{J L_r} (\varphi_{rd} i_{qs} - \varphi_{rq} i_{ds}) - \frac{1}{J} m_o \quad (2)$$

While ω_r is rotor speed, J is inertia and m_o is torque load.

The IFOC diagram based on three-phase IM shows in Fig. 1. The IFOC equations consist of rotor flux controller, current regulator (stator current controller in dq0 frame), and speed controller. The IFOC system has flux and electromagnetic torque commands. The torque command comes from the speed to torque equation shown in (4) with the speed command. The output of the IFOC system is a switching signal for the inverter while it requires feedback on the current and the rotor speed response of the three-phase induction motor. The IFOC equations are designed from the IM mathematical model. IFOC makes IM look like a DC motor due to the electromagnetic torque, and the rotor flux can be controlled separately.

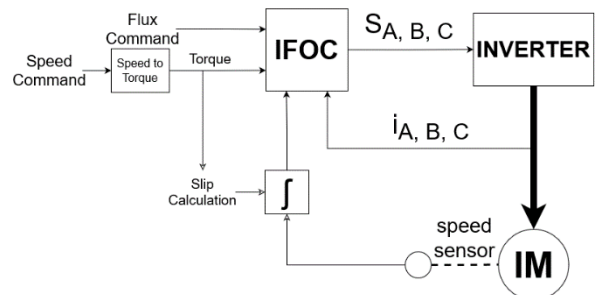


Fig.1. IFOC based three-phase IM

The rotor speed equation of IFOC shows in (3)

$$\frac{d\omega_r}{dt} = \frac{L_m}{J L_r} (\varphi_{rd} i_{qs}) - \frac{1}{J} m_o \quad (3)$$

While IM's electromagnetic torque (T_e) IM's electromagnetic torque (cap T sub e) is shown in (4).

$$T_e = \frac{3}{2} P \frac{L_m}{L_r} \varphi_{rd} i_{qs} \quad (4)$$

The correlation of the rotor speed and the electromagnetic torque is shown in (5).

$$\frac{d\omega_r}{dt} = \frac{2}{3 P J} T_e - \frac{1}{J} m_o \quad (5)$$

B. SMC

SMC is a model-based controller in which the control signal is designed from mathematical models of the systems. The SMC design consists of two subparts, i.e., the stable surface and the control law, to force the system states onto the chosen surface in a finite time shown in Fig. 3. The stable surface is designed in first-order using sliding surface (6) and the Lyapunov function (7) to guarantee the robustness and stability of the IFOC technique. The control law is designed using the sign function [8].

$$S(e) = \left[\frac{d}{dt} + \alpha \right]^{n-1} e \quad (6)$$

$$V = \frac{1}{2} S(e)^2 \quad (7)$$

where:

$S(e)$: sliding surface

V : Lyapunov function

e : error ($x_{command} - x_{feedback}$)

α, n : positive constant

The IFOC based IM controller in rotor speed using first-order SMC equation is determined in (8) [14].

$$U_c(T_e) = U_{eq}(T_e) + U_n \quad (8)$$

where:

$$U_{eq}(T_e) = \frac{3}{2} J P (\omega_r^* + \frac{m_o}{J})$$

$$U_n = K_{\omega_r} S_{\omega_r}(e_{\omega_r}) + \gamma_{\omega_r} \text{sign}(S_{\omega_r}(e_{\omega_r}))$$

with:

ω_r^* : speed command

$K_{\omega_r}, \gamma_{\omega_r}$: positive robustness constant (rotor speed)

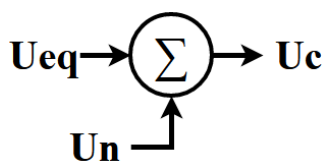


Fig.2. SMC design

C. Boundary-Layer Boundary-Layer

The sign function in first-order SMC causes a chattering phenomenon that harms the hardware and consumes more power to maintain the robustness [19], [20], [21], [22], [23]. This chattering phenomenon is due to the discontinuous control input shown in Fig. 3. (a). One of the most common methods of reducing the chattering phenomenon is the boundary layer approach. The boundary layer uses a continuous control input rather than discontinuous control input, namely a saturation function shown in Fig. 3. (b) and a hyperbolic tangent function shown in Fig. 3. (c) [24], [25], [26], [27]. The sign function in cap U sub n is replaced with saturation or hyperbolic tangent functions in the boundary layer approach. The sign function in U_n is

replaced with saturation or hyperbolic tangent functions in the boundary layer approach.

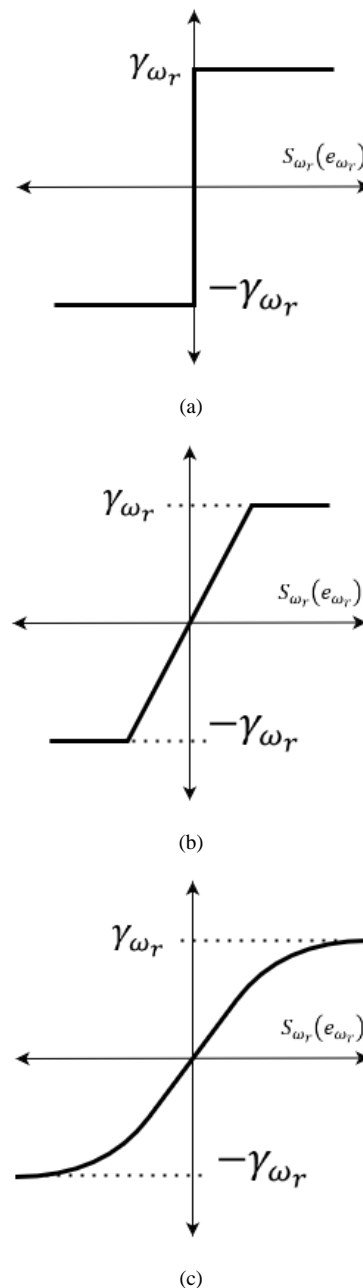


Fig.3. (a) sign function (b) saturation function (c) hyperbolic tangent function

The saturation function designed to control the rotor speed is given in (9).

$$\text{sat}(S_{\omega_r}(e_{\omega_r})) = \begin{cases} \text{sign}(S_{\omega_r}(e_{\omega_r})) & \text{for } |S_{\omega_r}(e_{\omega_r})| > BL \\ S_{\omega_r}(e_{\omega_r}) / \beta_{\text{layer}} & \text{for } |S_{\omega_r}(e_{\omega_r})| \leq BL \end{cases} \quad (9)$$

with β_{layer} is a positive constant of the the boundary layer (BL) using saturation function.

The hyperbolic tangent function used in this paper is expressed in (10). The boundary layer approximation performance is measured using the saturation and hyperbolic tangent function and hyperbolic tangent functions designed for rotor speed control (11).

$$\tanh(\tau x) = \frac{e^{\tau x} - e^{-\tau x}}{e^{\tau x} + e^{-\tau x}} \quad (10)$$

$$\begin{aligned} \tanh(S_{\omega_r}(e_{\omega_r})) = \\ \begin{cases} \text{sign}(S_{\omega_r}(e_{\omega_r})) & \text{for } |S_{\omega_r}(e_{\omega_r})| > BL \\ \tanh(\tau S_{\omega_r}(e_{\omega_r})) & \text{for } |S_{\omega_r}(e_{\omega_r})| \leq BL \end{cases} \quad (11) \end{aligned}$$

with τ is a positive constant of the the hyperbolic tangent function, which controls the shape of the function.

III. RESULT

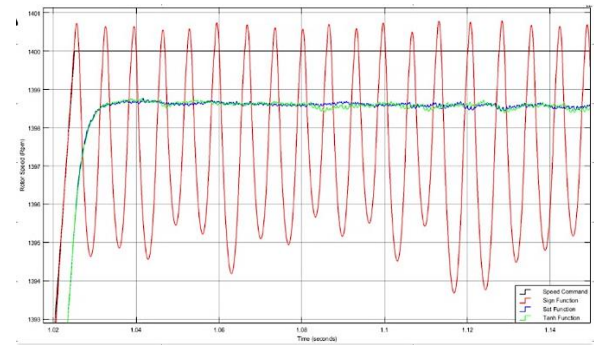
The IFOC-based IFOC-based IM is tested with a computer test using MATLAB/Simulink. The IFOC is implemented in a squirrel cage IM with parameters parameters shown in Table 1. The computer test uses $6 \cdot 10^{-5}$ seconds of sample time. The results consist of the performance of first-order SMC with sign function, saturation function, and hyperbolic tangent function designed in the speed controller.

Table 1. The parameter of IM

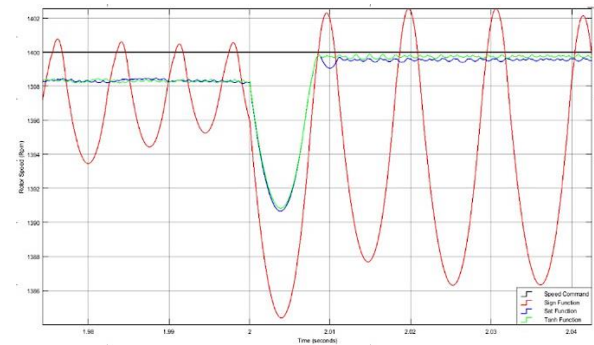
Frequency	f	50	Hz
Rotor Resistance	R_r	6.085	Ω
Stator Resistance	R_s	6.03	Ω
Rotor Inductance	L_r	0.4893	H
Stator Inductance	L_s	0.4893	H
Mutual Inductance	L_m	0.4503	H
Moment of Inertia	J	0.00488	Kg.m^2

A. Dynamic Response

The dynamics analysis of IFOC-based IFOC-based IM using SMC is presented for rotor speed response and stator current response in the dq0 frame. The rotor speed performance analysis in the transient and steady-state conditions is shown in Fig. 4. The step function, which is assumed to be a static disturbance, is given when the time is 2 seconds with a torque load of 2 Nm. The stator current response shown in Fig. 5 is depicted in the dq0 frame with various torque loads given at the start of the computer test.

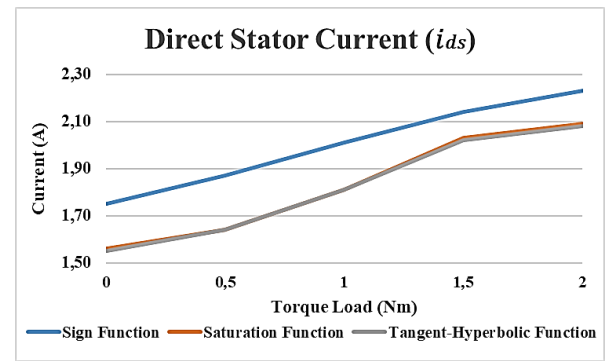


(a)

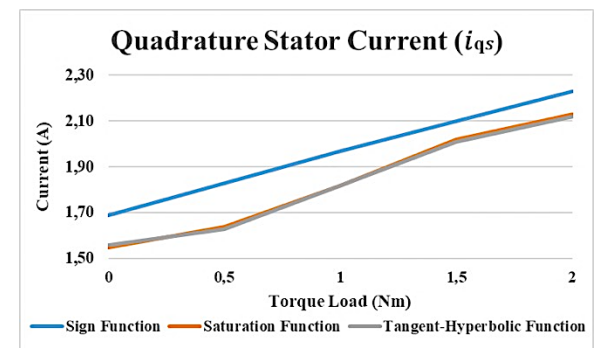


(b)

Fig.4. Rotor speed response (a) transient (b) under disturbance



(a)



(b)

Fig.5. Stator current response in dq0 frame (a) direct stator current (b) quadrature stator current

B. Power Response

The Power analysis measured active, reactive, and apparent power responses shown in Fig. 6. The Power is analyzed in various disturbances with constant speed

command. The speed command is designed for a high-speed response, making it easy to analyze controller performance. The active power of IFOC for IM calculates using (12) while the reactive power [19]

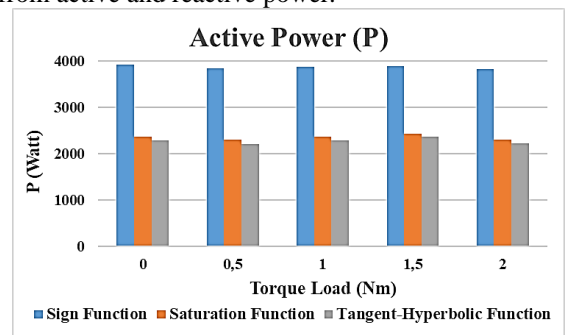
$$P = \frac{3}{2} (V_{ds}i_{ds} + V_{qs}i_{qs}) \quad (12)$$

$$Q = \frac{3}{2} (V_{qs}i_{ds} - V_{ds}i_{qs}) \quad (13)$$

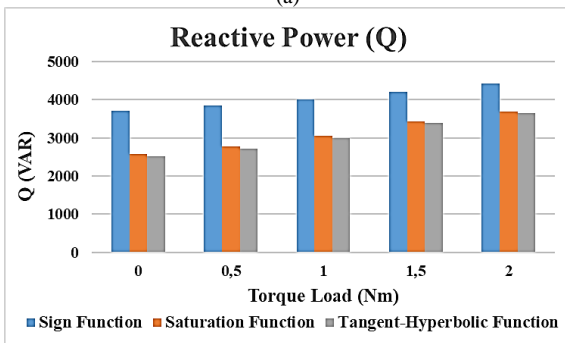
with :

- P : active power
- Q : reactive power.

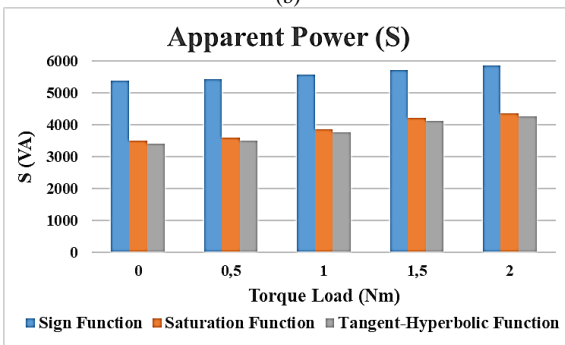
The power triangle equation calculates the apparent power (S) from active and reactive power. The power triangle equation calculates the apparent power (S) from active and reactive power.



(a)



(b)



(c)

Fig.6. Power response IFOC based IM (a) active power (b) reactive power (c) apparent power

IV. DISCUSSION

This section presents a test performed on on first-order SMC using sign function, saturation function, and hyperbolic tangent function. The performance of the boundary layer (saturation function and hyperbolic tangent function) was evaluated in rotor speed response. The boundary layer is placed in the rotor speed controller while the other uses first-order SMC. The

positive constant of the controller ($K_{\omega_r}, \gamma_{\omega_r}, \beta_{layer},$ and τ) is tuned intuitively. The computer testing for IFOC-based IFOC-based IM is done in two steps. The first step uses constant speed command at 1.400 rotations per minute with various torque loads at 2 seconds. The second step uses constant speed command at 1.400 rotations per minute with various torque loads given from the start of the test. The torque load is designed in 0,5 Nm, 1,0 Nm, 1,5 Nm, and 2,0 Nm.

The rotor speed response of IFOC-based IFOC-based IM using first-order SMC with sign function, saturation function, and hyperbolic tangent function in steady-state response and no-load condition has error steady-state less than 2% as shown in , as shown in the figure Fig. 3a. In overcoming the chattering phenomenon, the boundary layer performs better in the no-load condition than the without boundary layer. In overcoming the chattering phenomenon, the boundary layer performs better in the no-load condition than the without boundary layer. Fig 3b shows the sign function, saturation function, and hyperbolic tangent function to compensate under 2 Nm of disturbances. This response indicates indicates that the hyperbolic tangent function has the best performance. This chattering phenomenon makes a significant impact on power consumption and hardware lifespan. Fig. 4a and Fig. 4b show the reduction in direct and quadrature current consumption during the computer test. The saturation functions decrease 10.86% on direct current consumption while 8.28% on quadrature current consumption in no-load conditions. The hyperbolic tangent function has better performance in direct current with 11.43% of decreased current consumption. Besides, the hyperbolic tangent function's quadrature current consumption is just 7.69%. The saturation function's average decrease in immediate current consumption is 8.42% in varying load conditions, with a quadrature current consumption of 6.57%. Besides, the hyperbolic tangent function's quadrature current consumption is just 7.69%. The saturation function's average decrease in immediate current consumption is 8.42% in varying load conditions, with a quadrature current consumption of 6.57%. In hyperbolic tangent function, the direct current has 8.65%, with a quadrature current of 6.94%.

Table 2. Power and stator current reduction using saturation function

	Boundary Layer				
	Saturation Function				
	Torque Load (Nm)				
	0	0,5	1	1,5	2
P	39,46%	40,27%	38,81%	37,32%	39,94%
Q	30,16%	27,89%	24,00%	18,23%	16,59%
S	34,89%	33,79%	30,73%	26,41%	25,69%
i_{ds}	10,86%	12,30%	9,95%	5,14%	6,28%
i_{qs}	8,28%	10,38%	7,61%	3,81%	4,48%

Table 3. Power and stator current recent reduction using tangent-hyperbolic function

	Boundary Layer				
	Hyperbolic Tangent Function				
	Torque Load (Nm)				
	0	0,5	1	1,5	2
P	41,58%	42,46%	40,83%	39,30%	42,03%
Q	31,97%	29,58%	25,32%	19,39%	17,63%
S	36,85%	35,69%	32,34%	27,87%	27,06%
i_{ds}	11,43%	12,30%	9,95%	5,61%	6,73%
i_{qs}	7,69%	10,93%	7,61%	4,29%	4,93%

The boundary layer performance in reducing the chattering phenomenon shows in table 2 and table 3. Table 2 shows the performance of the the saturation function in reducing power and stator current with various torque loads. The active, reactive, and apparent power decreased decreased significantly. The hyperbolic tangent functions in reducing active, reactive, and apparent power are better than saturation functions, as shown in table 3. At no-load conditions, the hyperbolic tangent function increases the reduction in active power by 2.12%, reactive power by 1.81%, and apparent power by 1.97% compared to the saturation function. Under varying torque loads conditions (0.5 Nm, 1 Nm, 1.5 Nm, and 2 Nm), the hyperbolic tangent function still reduces the average active power consumption by 2.07%, and and reactive power consumption by by 1.30%, and apparent power consumption by 1.58%. In stator current response, the hyperbolic tangent function is slightly different from the saturation functions.

V. CONCLUSION CONCLUSION

This paper discusses the power efficiency of IFOC-based IFOC-based IM using first-order SMC with a boundary layer approach. The first-order SMC is designed in the the rotor speed controller, current regulator, and flux controller, while the rotor speed controller creates the boundary layer rotor speed controller creates the boundary layer. The boundary layer approach uses the saturation function and hyperbolic tangent function. The system test used a computer test that focussed on the chattering reduction in rotor speed response, stator current response in dq0 frame, and power analysis. The results show that that the hyperbolic tangent function has better power efficiency than the the saturation function at active, reactive, and apparent power.

ACKNOWLEDGMENT

This work was supported by Politeknik Elektronika Negeri Surabaya (PENS) and Politeknik Negeri Balikpapan (POLTEKBA).

REFERENCES

- [1] G. Sieklucki, "An Investigation into the Induction Motor of Tesla Model S Vehicle," dalam *2018 International Symposium on Electrical Machines (SME)*, Andrychow, Poland, 2018.
- [2] A. W. Aditya, Ihsan, R. M. Utomo and Hilmansyah, "Evaluasi Motor Listrik Sebagai Penggerak Mobil Listrik," *Jurnal Riset Sains dan Teknologi*, vol. 3, no. 2, pp. 55 - 59, 2019.
- [3] N. Rivière, M. Villani and M. Popescu, "Optimisation of a High Speed Copper Rotor Induction Motor for a Traction Application," dalam *IECON 2019 - 45th Annual Conference of the IEEE Industrial Electronics Society*, Lisbon, Portugal, 2019.
- [4] I. Yahyaoui and A. S. Cantero, "Scalar and Vector Control of Induction Motor for Online Photovoltaic Pumping," dalam *Advances in Renewable Energies and Power Technologies*, Elsevier, 2018, pp. 335 - 348.
- [5] A. Kumar, K. Gupta, H. Gupta and M. Kuber, "Development of Optimum Double Sided Linear Induction Motor for Military Application," dalam *2020 IEEE International Conference on Power Electronics, Drives and Energy Systems (PEDES)*, Jaipur, India, 2020.
- [6] K. Tshiloz and S. Djurovic, "Scalar controlled induction motor drive speed estimation by adaptive sliding window search of the power signal," *Electrical Power and Energy Systems*, pp. 80 - 91, 2017.
- [7] P. Vladimir and S. Dmitry, "To Issue of Designing Scalar Closed-Loop Controllers for Frequency Controlled Induction Motor Drives," dalam *2018 17th International Ural Conference on AC Electric Drives (ACED)*, Ekaterinburg, Russia , 2018.
- [8] A. W. Aditya, D. C. Happyanto and B. Sumantri, "Boundary-Layer Effect in Robust Sliding Mode Control for Indirect Field Oriented Control of 3-Phase Induction Motor," *International Journal on Electrical Engineering and Informatics*, vol. 12, no. 2, pp. 188 - 204, 2020.
- [9] P. K. Behera, M. K. Behera and A. K. Sahoo, "Speed Control of Induction Motor using Scalar Control Technique," dalam *International Conference on Emergent Trends in Computing and Communication (ETCC-2014)*, 2014.

- [10] P. C. Valencia-Manrique and R. J. Coaquira-Castillo, "Speed Performance Comparative of Indirect Field Oriented Control based on current model for Induction Motors in Educational Equipment," dalam *2020 IEEE XXVII International Conference on Electronics, Electrical Engineering and Computing (INTERCON)*, Lima, Peru, 2020.
- [11] A. W. Aditya, Ihsan, R. M. Utomo and Hilmansyah, "Pemodelan State Space Motor Induksi Tiga Fasa Sebagai Penggerak Mobil Listrik," *Jurnal Teknologi*, vol. 12, no. 1, pp. 39 - 48, 2020.
- [12] Y. B. Zbede, S. M. Gadoue and D. J. Atkinson, "Model Predictive MRAS Estimator for Sensorless Induction Motor Drives," *IEEE Transactions on Industrial Electronics*, vol. 63, no. 6, pp. 3511-3521, 2016.
- [13] H. H. Fakhruddin, H. Toar, E. Purwanto, H. Oktavianto, R. A. N. Apriyanto and A. W. Aditya, "Kendali Kecepatan Motor Induksi 3 Fase Berbasis Particle Swarm Optimization (PSO)," *ELKOMIKA: Jurnal Teknik Energi Elektrik, Teknik Telekomunikasi, & Teknik Elektronika*, vol. 8, no. 3, pp. 477 - 491, 2020.
- [14] A. W. Aditya, D. C. Happyanto and B. Sumantri, "Application of Sliding Mode Control in Indirect Field Oriented," *EMITTER International Journal of Engineering Technology Control (IFOC) for Model Based Controller*, vol. 5, no. 2, pp. 255 - 269, 2017.
- [15] M. Aktas, K. Awaili, M. Ehsani and A. Arisoy, "Direct torque control versus indirect field-oriented control of induction motors for electric vehicle applications," *Engineering Science and Technology, an International Journal*, vol. 23, no. 5, pp. 1134-1143, 2020.
- [16] Y. Liu, W. Yan, D. Xu, W. Yang and W. Zhang, "Direct Torque Control of PMSM Based on Model Free iPI Controller," dalam *2018 IEEE 7th Data Driven Control and Learning Systems*, Enshi, Hubei Provinc, 2018.
- [17] D. Na and H. Xue-shuo, "Model-free controller design for advanced energy-saving control of the refrigeration system," dalam *2016 35th Chinese Control Conference (CCC)*, Chengdu, China, 2016.
- [18] H. Lihong, L. Ke and W. Hongyu, "Research on application of boost converter based on data-driven full-format model-free adaptive controller," dalam *2016 Chinese Control and Decision Conference (CCDC)*, Yinchuan, China, 2016.
- [19] A. W. Aditya, M. R. Rusli, B. Praharsena, E. Purwanto and D. C. Happyanto, "The Performance of FOSMC and Boundary – SMC in Speed Controller and Current Regulator for IFOC-Based Induction Motor Drive," dalam *2018 International Seminar on Application for Technology of Information and Communication (iSemantic)*, Semarang, Indonesia, 2018.
- [20] A. W. Aditya, R. M. Utomo, Hilmansyah, E. Purwanto, M. R. Rusli and B. Praharsena, "Power performance of boundary technique on FOSMC based induction motor drives," dalam *The 2nd International Conference on Applied Science and Technology (iCAST)*, Bali, Indonesia, 2019.
- [21] B. Sumantri, N. Uchiyama and S. Sano, "Least square based sliding mode control for a quad-rotor helicopter and energy saving by chattering reduction," *Mechanical Systems and Signal Processing*, Vol. %1 dari %266 - 67, pp. 768 - 784, 2016.
- [22] K. Swathi and G. N. Kumar, "Design of intelligent controller for reduction of chattering phenomenon in robotic arm: A rapid prototyping," *Computers & Electrical Engineering*, vol. 74, pp. 483-497, 2019.
- [23] I. Castillo and L. B. Freidovich, "Describing-function-based analysis to tune parameters of chattering reducing approximations of Sliding Mode controllers," *Control Engineering Practice*, vol. 95, 2020.
- [24] I. E. Makrini, C. Rodriguez-Guerrero, D. Lefeber and B. Vanderborght, "The Variable Boundary Layer Sliding Mode Control: A Safe and Performant Control for Compliant Joint Manipulators," *IEEE Robotics and Automation Letters*, vol. 2, no. 1, pp. 167 - 192, 2017.
- [25] Y. K. Kim and C. H. Paek, "Position Error Reduction of the Actuator Using the Sliding Mode Controller with Variable Boundary Layer Thickness," dalam *SICE-ICASE International Joint Conference 2006*, Busan, Korea, 2006.
- [26] M. Mancini, E. Capello and E. Punta, "Sliding Mode Control with Chattering Attenuation and Hardware Constraints in Spacecraft Applications," dalam *21st the International Federation of Automatic Control (IFAC) World Congress*, Berlin, Germany, 2020.
- [27] J. R. B. A. Monteiro, C. M. R. Oliveira and M. L. Aguiar, "Sliding mode control of brushless DC motor speed with chattering reduction," dalam *2015 IEEE 24th International Symposium on Industrial Electronics (ISIE)*, Buzios, Brazil, 2015.